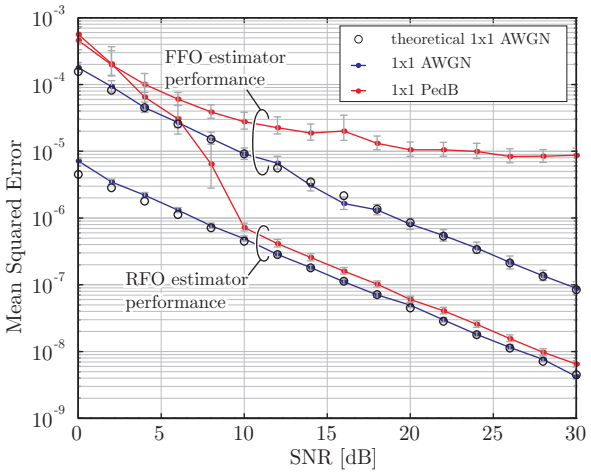

Fig. 3. Calculated and simulated Mean Squared Error for FFO and RFO in 1×1 transmission.

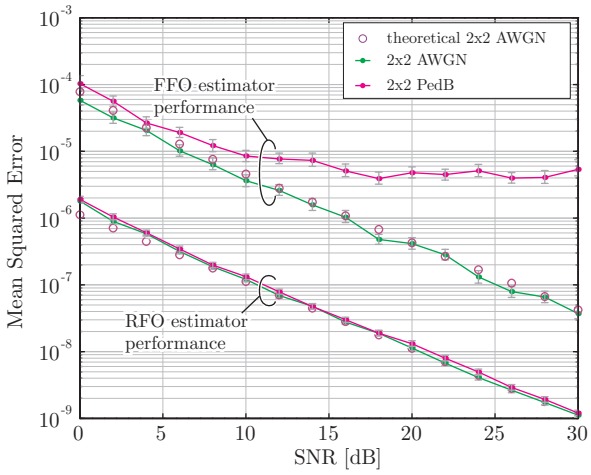

Fig. 4. Calculated and simulated Mean Squared Error for FFO and RFO in 4×2 transmission.

transmission. According to [14], sampling frequencies on both ends are assumed to be perfectly synchronized. The other simulation parameters are listed in Table I. Using the bootstrap algorithm [15] we calculated the 95% confidence intervals for all simulated curves. These intervals are indicated by the vertical bars in the simulated curves.

A. Estimation Performance

The estimation performance is presented in Fig. 3, Fig. 4 and Fig. 5 in terms of MSE for the FFO/RFO and error probability for the IFO. In the simulated 1000 subframes transmission, FFO and IFO estimations are carried out in every fifth subframe, leading to a relatively large confidence interval compared to the RFO estimation curves.

In Fig. 3 and Fig. 4, it is shown that for AWGN transmission, the simulated curves agree quite well with the calculated theoretical MSE. For ITU Pedestrian B (PedB) [12] channels with time dispersion, the MSE of the FFO estimator saturates around 10^{-5} since the beginning of the CP is corrupted by the delayed version of the previous OFDM symbol. As long as the FFO estimation error does not exceed the estimation range of the RFO estimator, this does not affect the overall estimation performance.

For the IFO estimation, errors only occur for the SISO transmission in PedB channel (Fig. 5). The error in the IFO estimation results in a subcarrier mismatch which fails the RFO estimation where correct reference symbol extraction is required (Fig 3, SNR < 10 dB).

B. System Performance

In order to investigate the impact of the CFO on the system performance when no CFO compensation is employed, we introduced 100 logarithmically spaced CFOs between 10^{-4} and 10^{-1} subcarrier spacings and observe the variation of the physical layer coded throughput for a series of CQI values (Fig. 6 and Fig. 7). The simulated throughput curves drop sharply when the CFOs reach certain levels. The higher CQIs

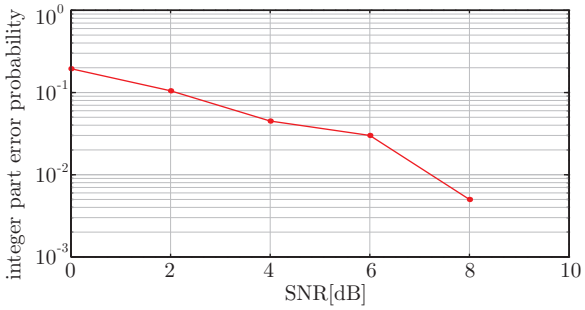

Fig. 5. Error probability of the IFO estimation.

which have larger modulation scheme and higher coding rate also require more accurate frequency synchronization.

The uncoded Bit Error Ratio (BER) curves for simulations in AWGN and PedB channels are shown in Fig. 8 and Fig. 9. When comparing to the perfect synchronization cases, both 1×1 SISO and 4×2 MIMO transmission show hardly any loss. The same trend is observed for the coded throughput curves in Fig. 10.

Note that CQI 15, which has the most demanding requirements on CFO compensation, requires the CFO to be less than about 10^{-3} (see Fig. 6) which corresponds to 10^{-6} of MSE. This requirement is fullfilled by our CFO compensation scheme at SNR 30 dB (see Fig. 3), explaining the negligible loss in the simulated BER and throughput curves.

VI. Conclusion

In this paper, a CFO compensation scheme for 3GPP LTE is presented and evaluated. Simulation results show that the presented three stage scheme is sufficient to compensate even relatively large CFOs in slow fading scenarios. Compared to perfect synchronization, the performance loss is hardly noticeable. Since the synchronization and reference signals in the standard are not dedicated for carrier frequency syn-

Fig. 6. Throughput of SISO transmission over an AWGN channel when CFO is introduced.

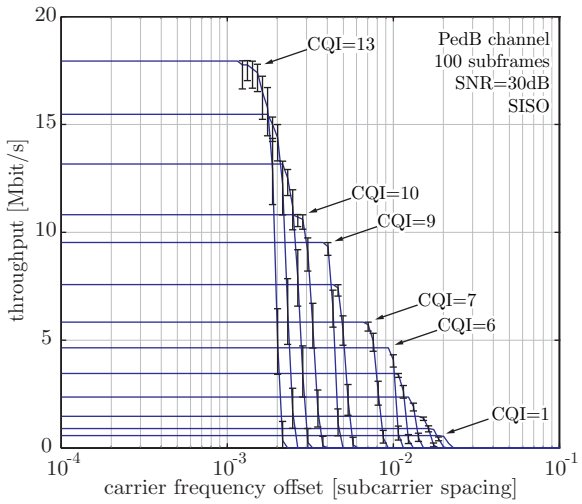

Fig. 7. Throughput of SISO transmission over a PedB channel when CFO is introduced.

chronization but mainly used for cell search and channel estimation, it is not necessary to apply more sophisticated compensation schemes to reduce the resource overhead. We plan further investigation in high mobility scenarios with fast fading channels.

Acknowledgments

Funding for this research was provided by the fFORTE WIT - Women in Technology Program of the Vienna University of Technology. This program is co-financed by the Vienna University of Technology, the Ministry for Science and Research and the fFORTE Initiative of the Austrian Government. Also, this work has been co-funded by the Christian Doppler Laboratory for Wireless Technologies for Sustainable Mobility.

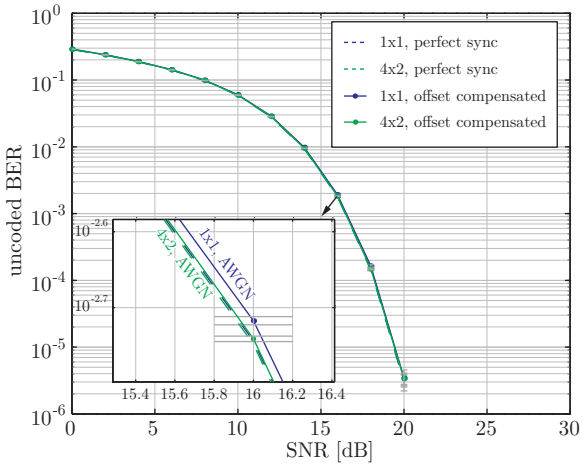

Fig. 8. Uncoded BER of CQI=9 SISO transmission in AWGN channel.

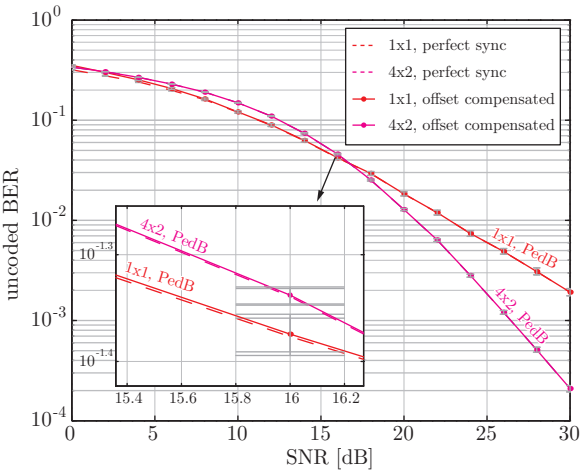

Fig. 9. Uncoded BER of CQI=9 SISO transmission in PedB channel.

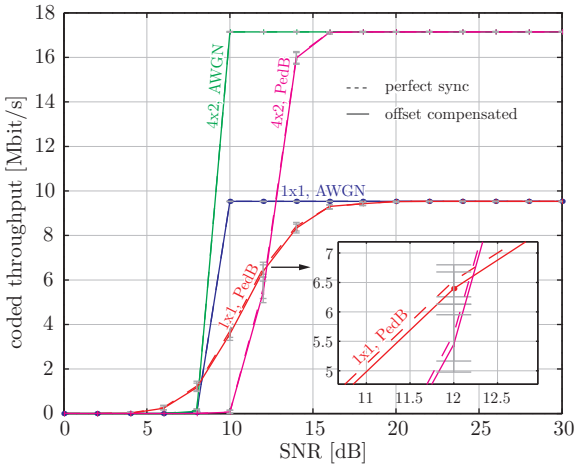

Fig. 10. Coded Throughput of CQI=9 SISO/MIMO transmission over AWGN and PedB channel.

APPENDIX I. DERIVATION OF THE THEORETICAL MSE OF THE FFO ESTIMATOR

In order to derive the theoretical MSE of the FFO estimator, we rewrite Eq. (5) as

$$\hat{\varepsilon}_{\text{FFO}} = -\frac{1}{2\pi}\arctan\frac{\Im\left\{\sum_{m=1}^{N_\text{R}}\sum_{l=1}^{N_\text{f}}\sum_{n=1}^{N_\text{g}} r_{l,n}^{(m)} r_{l,n+N}^{(m)*}\right\}}{\Re\left\{\sum_{m=1}^{N_\text{R}}\sum_{l=1}^{N_\text{f}}\sum_{n=1}^{N_\text{g}} r_{l,n}^{(m)} r_{l,n+N}^{(m)*}\right\}}, \tag{11}$$

where $\Re\{\cdot\}$ and $\Im\{\cdot\}$ are the real and imaginary operators. The estimation error can be written as

$$\begin{aligned}&\varepsilon_{\text{FFO}} - \hat{\varepsilon}_{\text{FFO}} = \\ =&\frac{1}{2\pi}\arctan\frac{\Im\left\{\sum_{m=1}^{N_\text{R}}\sum_{l=1}^{N_\text{f}}\sum_{n=1}^{N_\text{g}} r_{l,n}^{(m)} r_{l,n+N}^{(m)*} e^{j2\pi\varepsilon_{\text{FFO}}}\right\}}{\Re\left\{\sum_{m=1}^{N_\text{R}}\sum_{l=1}^{N_\text{f}}\sum_{n=1}^{N_\text{g}} r_{l,n}^{(m)} r_{l,n+N}^{(m)*} e^{j2\pi\varepsilon_{\text{FFO}}}\right\}}.\end{aligned} \tag{12}$$

When the error is small, Eq. (12) can be approximated to

$$\begin{aligned}&\varepsilon_{\text{FFO}} - \hat{\varepsilon}_{\text{FFO}} \cong \\ \cong&\frac{1}{2\pi}\frac{\Im\left\{\sum_{m=1}^{N_\text{R}}\sum_{l=1}^{N_\text{f}}\sum_{n=1}^{N_\text{g}} r_{l,n}^{(m)} r_{l,n+N}^{(m)*} e^{j2\pi\varepsilon_{\text{FFO}}}\right\}}{\Re\left\{\sum_{m=1}^{N_\text{R}}\sum_{l=1}^{N_\text{f}}\sum_{n=1}^{N_\text{g}} r_{l,n}^{(m)} r_{l,n+N}^{(m)*} e^{j2\pi\varepsilon_{\text{FFO}}}\right\}}.\end{aligned} \tag{13}$$

In order to find the real and imaginary terms, we rewrite Eq. (1) for simplicity

$$r_{l,n}^{(m)} = \left(\dot{r}_{l,n}^{(m)} + v_{l,n}^{(m)}\right) e^{j2\pi\hat{\varepsilon}_{\text{FFO}}(n+l(N+N_\text{g}))/N}, \tag{14}$$

with $\dot{r}_{l,n}^{(m)} = x_{l,n}^{(m)} * h_{l,n}^{(m)}$ denoting the received signal without CFO. Thus, we have

$$\begin{aligned}&r_{l,n}^{(m)} r_{l,n+N}^{(m)*} e^{j2\pi\varepsilon_{\text{FFO}}} = \\ =&\left(\dot{r}_{l,n}^{(m)} + v_{l,n}^{(m)}\right)\left(\dot{r}_{l,n+N}^{(m)} + v_{l,n+N}^{(m)}\right)^* e^{j2\pi(\varepsilon_{\text{FFO}}-\hat{\varepsilon}_{\text{FFO}})} \\ =&\left(\dot{r}_{l,n}^{(m)}\dot{r}_{l,n+N}^{(m)*} + \dot{r}_{l,n}^{(m)} v_{l,n+N}^{(m)*} + v_{l,n}^{(m)}\dot{r}_{l,n+N}^{(m)*} + v_{l,n}^{(m)} v_{l,n+N}^{(m)*}\right) \\ &\cdot \underbrace{e^{j2\pi(\varepsilon_{\text{FFO}}-\hat{\varepsilon}_{\text{FFO}})}}_{\approx 1 \text{ for small error}}.\end{aligned} \tag{15}$$

When relatively large SNR is assumed, there is

$$\begin{aligned}\Re\left\{\dot{r}_{l,n}^{(m)}\dot{r}_{l,n+N}^{(m)*}\right\} \gg& \Re\left\{\dot{r}_{l,n}^{(m)} v_{l,n+N}^{(m)*} + v_{l,n}^{(m)}\dot{r}_{l,n+N}^{(m)*}\right. \\ &\left. + v_{l,n}^{(m)} v_{l,n+N}^{(m)*}\right\}.\end{aligned} \tag{16}$$

Thus, the denominator in Eq. (13) becomes

$$\begin{aligned}&\Re\left\{\sum_{m=1}^{N_\text{R}}\sum_{l=1}^{N_\text{f}}\sum_{n=1}^{N_\text{g}} r_{l,n}^{(m)} r_{l,n+N}^{(m)*} e^{j2\pi\varepsilon_{\text{FFO}}}\right\} \\ =&\sum_{m=1}^{N_\text{R}}\sum_{l=1}^{N_\text{f}}\sum_{n=1}^{N_\text{g}} \dot{r}_{l,n}^{(m)}\dot{r}_{l,n+N}^{(m)*} = N_\text{R} N_\text{f} N_\text{g}\sigma_r^2,\end{aligned} \tag{17}$$

where σ_r^2 is the average signal power of the received signal in time domain.

Based on the fact that $E\{v_{l,n}^{(m)}\} = 0$, $E\{|v_{l,n}^{(m)}|^2\} = \sigma_v^2$, the variance of the nominator in Eq. (13) can be found by straightforward calculation:

$$E\{|\Im\{\cdot\}|^2\} = N_\text{R} N_\text{f} N_\text{g}\left(\sigma_v^2\sigma_r^2 + \frac{1}{2}\sigma_v^4\right) \tag{18}$$

Therefore, the MSE is given by

$$\begin{aligned}&E\{|\varepsilon_{\text{FFO}} - \hat{\varepsilon}_{\text{FFO}}|^2\} = \frac{1}{4\pi^2}\frac{E\{|\Im\{\cdot\}|^2\}}{(N_\text{R} N_\text{f} N_\text{g}\sigma_r^2)^2} = \frac{2\sigma_v^2\sigma_r^2 + \sigma_v^4}{8\pi^2 N_\text{R} N_\text{g} N_\text{f}\sigma_r^4} \\ =&\frac{2\gamma_t + 1}{8\pi^2 N_\text{R} N_\text{g} N_\text{f}\gamma_t^2} \approx \frac{1}{4\pi^2 N_\text{R} N_\text{g} N_\text{f}\gamma_t},\end{aligned} \tag{19}$$

where $\gamma_t = \sigma_r^2/\sigma_v^2 \gg 1$ is the signal-to-noise ratio of the received signal in time domain.

REFERENCES

[1] 3GPP, "Technical specification group radio access network; (E-UTRA) and (E-UTRAN); overall description; stage 2," Tech. Rep., 2008. [Online]. Available: http://www.3gpp.org/ftp/Specs/html-info/36300.htm

[2] P. H. Moose, "A technique for orthogonal frequency division multiplexing frequency offset correction," *IEEE Transactions on Communications*, vol. 42, no. 10, pp. 2908–2914, Oct 1994.

[3] J. J. van de Beek, M. Sandell, and P. O. Borjesson, "ML estimation of time and frequency offset in OFDM system," *IEEE Transactions on Signal Processing*, vol. 45, pp. 1800–1805, Jul. 1997.

[4] M. Speth, S. Fechtel, G. Fock, and H. Meyr, "Optimum receiver design for OFDM-based broadband transmission. II. a case study," *IEEE Transactions on Communications*, vol. 49, pp. 571–578, Apr 2001.

[5] D. Toumpakaris, J. Lee, and H. Lou, "Estimation of integer carrier frequency offset in OFDM systems based on the maximum likelihood principle," *IEEE Transactions on Broadcasting*, vol. 55, pp. 95–108, March 2009.

[6] Q. Wang, C. Mehlführer, and M. Rupp, "SNR optimized residual frequency offset compensation for WiMAX with throughput evaluation," in *Proc. 17th European Signal Processing Conference (EUSIPCO 2009)*, Glasgow, Scotland, Aug. 2009.

[7] Q. Wang, S. Caban, C. Mehlführer, and M. Rupp, "Measurement based throughput evaluation of residual frequency offset compensation in WiMAX," in *Proc. 51st International Symposium ELMAR-2009*, Zadar, Croatia, Sep. 2009.

[8] C. R. N. Athaudage and K. Sathananthan, "Cramer-rao lower bound on frequency offset estimation error in OFDM systems with timing error feedback compensation," in *Proc. 5th International Conference on information, Communications and Signal Processing*, Bangkok, Thailand, Dec. 2005.

[9] K. Manolakis, D. M. Gutierrez Estevez, V. Jungnickel, W. Xu, and C. Drewes, "A closed concept for synchronization and cell search in 3GPP LTE systems," in *Proc. IEEE Wireless Communication and Networking Conference (WCNC)*, Budapest, Hungary, 2009.

[10] C. Mehlführer, M. Wrulich, J. C. Ikuno, D. Bosanska, and M. Rupp, "Simulating the long term evolution physical layer," in *Proc. 17th European Signal Processing Conference (EUSIPCO 2009)*, Glasgow, Scotland, UK, Aug. 2009. [Online]. Available: http://publik.tuwien.ac.at/files/PubDat_175708.pdf

[11] 3GPP, "Technical specification group radio access network; (E-UTRA) and (E-UTRAN); physical channels and modulation; (release 8)," Tech. Rep., 2008. [Online]. Available: http://www.3gpp.org/ftp/Specs/html-info/36211.htm

[12] "Recommendation ITU-R M.1225: Guidelines for evaluation of radio transmission technologies for IMT-2000," Tech. Rep., 1997.

[13] "LTE simulator homepage." [Online]. Available: http://www.nt.tuwien.ac.at/ltesimulator/

[14] B. Stantchev and G. Fettweis, "Time-variant distortion in OFDM," *IEEE Communications Letters*, vol. 4, pp. 312–314, Oct 2000.

[15] B. Efron and D. V. Hinkley, *An Introduction to the Bootstrap (CRC Monographs on Statistics & Applied Probability 57)*, 1st ed. Chapman & Hall/CRC, 1994.